IEEE Access
Multidisciplinary | Rapid Review | Open Access Journal

Received November 23, 2018, accepted December 22, 2018, date of publication December 27, 2018,
date of current version January 16, 2019.

Digital Object Identifier 10.1109/ACCESS.2018.2889849

Adaptive Interaction Controller for Compliant Robot Base Applications

LORIS ROVEDA, (Fellow, IEEE)
Institute of Intelligent Industrial Technologies and Systems for Advanced Manufacturing, Italian National Research Council, 20133 Milan, Italy
e-mail: loris.roveda@stiima.cnr.it

This work was supported by the H2020 CleanSky 2 through the Project EURECA under Grant 738039.

ABSTRACT The aim of this paper is to design an adaptive interaction controller to deal with compliant base robotic systems executing interaction tasks (e.g., assembly tasks). The main goal of such controller is to avoid the force-overshoots while compensating the robot base dynamics. The proposed controller does not require any modeling/estimation of the environment dynamics, neither of the compliant robot base dynamics. In fact, based on the impedance control, the proposed controller is capable to online adapt its parameters to track a reference force. The stability of the proposed controller has been proven. The proposed controller has been applied to an industrial scenario. In particular, an assembly task has been selected to validate the control performance. A KUKA iiwa 14 R820 manipulator mounted on a compliant robot base (implementing different dynamic behaviors) and equipped with a Robotiq gripper has been used. The experimental results show the achieved control performance. The results have also been compared with the previous designed control methods.

INDEX TERMS Adaptive interaction control, compliant robot base, force overshoots avoidance, impedance control, industrial application.

I. INTRODUCTION

The use of industrial lightweight robots in industrial interaction tasks (such as assembly tasks) is increasing. In fact, such robots allow to establish a safe and controlled interaction with the environment [1]. Additionally, in order to improve the flexibility of the industrial plant, such manipulators are often mounted on mobile structures [2]. Such mountings cannot be considered as rigid, and introduce a degree of elasticity at the robot base, affecting the interaction dynamics [3].

A. INTERACTION CONTROL

Impedance [4], [5] based controllers can be adopted in order to implement a required robot dynimics while allowing the tracking of a specific position/force. Many works have been developed adapting the impedance control parameters (*i.e.*, setpoint, stiffness and damping) on the basis of the robot measurements (*i.e.*, poitions/velocities and/or forces). Such algorithms can be divided in two main approaches: (a) set-point deformation [6]–[8] and (b) variable impedance adaptation [8]–[10].

While in class (a) algorithms the impedance control setpoint is modified on the base of the estimated environment stiffness and of the force-tracking error, in class (b) methods introduce the modification of the impedance parameters during the task execution, mainly exploiting gain-scheduling strategies that select the stiffness and damping parameters from a pre-calculated set on the basis of the current state of the robot. Commonly, (a) approaches maintain a constant dynamic behavior of the robot (resulting in limited controllers bandwidth). (b) approaches are used in tasks with a stationary, known and structured environment, adapting the bandwidth of the controllers on the basis of the measured interaction.

B. COMPENSATION OF THE ROBOT BASE DYNAMICS

Compliant robot base applications (including mobile platforms) are deeply investigated in order to formalize control schemas and the design of applications [11], [12]. The adoption of lightweight robots mounted on such platforms is also relevant in order to interact with the surrounding environment [13]–[15]. In such scenario, the robot base dynamics compensation is necessary to avoid any instability or force overshoot, allowing to achieve high-precise interaction control. Some works take into account compliant robot bases in order to suppress any undesired oscillation at the robot

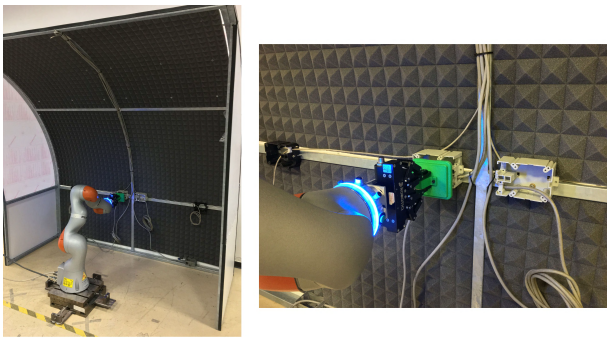

FIGURE 1. Experimental setup for the proposed adaptive interaction controller validation. The proposed setup involves a KUKA iiwa 14 R820 manipulator mounted on a compliant base. The target industrial application is related to the H2020 CleanSky 2 EURECA project, in which the manipulator has to install with high-precision compliant components in the aircraft cabin scenario.

end-effector [16]–[18]. However, such works do not deal with force-tracking performance. Other works investigate interaction tasks in order to guarantee smooth transition from a free-space motion to contact with an unknown environment [19] or to tune the manipulator stiffness to the target one [20], [21]. However, no work investigates the important issue of avoid force overshoots while taking into account the robot base elasticity.

C. WORK CONTRIBUTION

Authors have already investigated such control applications, both considering a fixed robot base [1], [8], [22]–[24] and a compliant robot base [14], [25], [26]. However, a linear dynamics has been considered in all the papers, requiring its parameters identification using additional external sensors.

In order to avoid any modeling/identification of the interacting environment, neither of the robot base, the aim of this paper is to design an adaptive interaction controller to track a reference interaction force achieving the avoidance of any overshoots during the task execution. Based on the impedance control, the proposed controller is capable to on-line adapt its parameters (a proportional force-tracking control gain and a derivative damping control gain) on the basis of the measured force, the force reference and the filtered force reference (shaping the bandwidth of the closed-loop system). The stability of the proposed controller has been derived considering a linear coupled dynamic system. The proposed controller has been applied to an industrial application. In particular, considering the H2020 CleanSky 2 EURECA project, an assembly task has been selected. A KUKA iiwa 14 R820 manipulator mounted on a compliant robot base (implementing linear/non linear dynamics) and equipped with a Robotiq gripper has been used. Experimental results show the avoidance of force-overshoots while achieving the target bandwidth. Results have been also compared with previous designed control methods, highlighting the improved performance.

II. CONTROLLER DESIGN

The proposed controller is composed by two control loops: an internal impedance controller and an external adaptive interaction controller. In the following, both the control loops are described.

A. CARTESIAN IMPEDANCE CONTROL DYNAMICS

General Notation

$\mathbf{M}_t, \mathbf{M}_\varphi$: translational and rotational impedance control inertia matrix

$\mathbf{D}_t, \mathbf{D}_\varphi$: translational and rotational impedance control damping matrix

$\mathbf{K}_t, \mathbf{K}_\varphi$: translational and rotational impedance control stiffness matrix

$\mathbf{f}_t, \boldsymbol{\mu}^d$: Cartesian external forces and Cartesian external torques vectors referred to the target frame

$\Delta\mathbf{p} = \mathbf{p}^d - \mathbf{p}$: difference between reference and measured Cartesian translations

$\boldsymbol{\varphi}_{cd}$: set of Euler angles extracted from $\mathbf{R}_c^d = \mathbf{R}_d^T\mathbf{R}_c$, describing the mutual orientation between the compliant frame (at the end-effector) and the target frame

$\mathbf{S}_\omega(\boldsymbol{\varphi}_{cd})$: transformation from Euler angles derivatives to angular velocities $\boldsymbol{\omega} = \mathbf{S}_\omega(\boldsymbol{\varphi}_{cd})\dot{\boldsymbol{\varphi}}_{cd}$ [27]

$\mathbf{M}_r, \mathbf{D}_r, \mathbf{K}_r, \mathbf{f}_r, \Delta\mathbf{x}_r$: impedance matrices composed by both the traslational and rotational parts

As described in [28], on the basis of the robot dynamics, it is possible to design the Cartesian impedance control. In particular, the reference Cartesian acceleration $\ddot{\mathbf{x}} = [\ddot{\mathbf{p}}; \ddot{\boldsymbol{\varphi}}_{cd}]$ (where $\ddot{\mathbf{p}}$ is the reference traslational acceleration, and $\ddot{\boldsymbol{\varphi}}_{cd}$ is the reference angular acceleration) can be defined as:

$$\begin{aligned}\ddot{\mathbf{p}} &= \mathbf{M}_t^{-1}\left(-\mathbf{D}_t\dot{\mathbf{p}} - \mathbf{K}_t\,\Delta\mathbf{p} - \mathbf{f}_t\right)\\ \ddot{\boldsymbol{\varphi}}_{cd} &= \mathbf{M}_\varphi^{-1}\left(-\mathbf{D}_\varphi\,\dot{\boldsymbol{\varphi}}_{cd} - \mathbf{K}_\varphi\,\boldsymbol{\varphi}_{cd} + \mathbf{S}_\omega^T(\boldsymbol{\varphi}_{cd})\,\boldsymbol{\mu}^d\right)\end{aligned} \quad (1)$$

The equivalent Cartesian behaviour of the controlled robot results in:

$$\mathbf{M}_r\,\ddot{\mathbf{x}}_r + \mathbf{D}_r\,\dot{\mathbf{R}}_r + \mathbf{K}_r\,\Delta\mathbf{x}_r = \mathbf{f}_r \quad (2)$$

The KUKA iiwa 14 R820 enables a task space visco-elastic behavior (as for the previous KUKA LWR 4+ manipulator [29]), with decoupled tunable stiffness and damping $\mathbf{K}_r := diag(K_{r,x}, K_{r,y}, K_{r,z}, K_{r,\varphi_x}, K_{r,\varphi_y}, K_{r,\varphi_z})$, $\mathbf{D}_r := diag(D_{r,x}, D_{r,y}, D_{r,z}, D_{r,\varphi_x}, D_{r,\varphi_y}, D_{r,\varphi_z})$. The robot $\mathbf{M}_r := diag(M_{r,x}, M_{r,y}, M_{r,z}, M_{r,\varphi_x}, M_{r,\varphi_y}, M_{r,\varphi_z})$ mass and inertia parameters can be experimentally identificated by following the procedure proposed in [30]. In particular, a position chirp has been imposed to the impedance control set-point $\mathbf{x}_r^0$ and the robot Cartesian position $\mathbf{x}_r$ has been measured. The range of frequencies considered is $0 - 5.5\ Hz$. Only the main task direction X (see Section IV) has been investigated. However, the procedure can be applied to any Cartesian

direction separatelly (since the Cartesian impedance control decouples the Cartesian degree of freedom - DoFs). The H_1 estimator has been used to evaluate the frequency response function (FRF) of the controlled robot:

$$H_1 = \frac{G_{xy}}{G_{xx}} \tag{3}$$

where x is the input signal (*i.e.*, the imposed impedance control set-point $x^0_{r,x}$), y the output signal (*i.e.*, the measured robot Cartesian position $x_{r,x}$), G_{xy} the cross-power spectrum between input and output signals, G_{xx} the auto spectrum of the input signal. The H_1 estimator has been selected due to the high noise on the output signal.

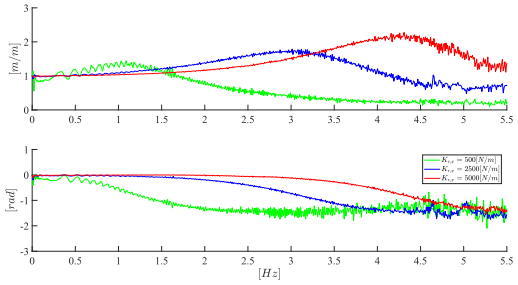

FIGURE 2. Frequency response functions estimated for the KUKA iiwa 14 R820 manipulator in impedance control. The plot shows the modification of the robot dynamics on the basis of the imposed stiffness $K_{r,x}$ parameter.

Three values for the impedance control stiffness $K_{r,x}$ has been imposed: 500 $[N/m]$, 2500 $[N/m]$, 5000 $[N/m]$, while the damping ration $h_{r,x}$ (defining the damping $D_{r,x} = 2\,h_{r,x}\sqrt{K_{r,x}M_{r,x}}$) has been imposed equal to 0.5. The identified FRFs are shown in Figure 2. In particular, the natural frequencies f_N of the controlled robot, varying together with the impedance control stiffness parameter, can be measured in order to calculate the impedance control mass $M_{r,x} = K_r/(2\pi f_N)^2$. The estimation of the mass parameters are shown in Tables 1 and such values are necessary to implement the external adaptive interaction control loop described in the following section.

TABLE 1. Estimated mass parameters.

Mass $M_{r,x}$ $[kg]$		
$K_{r,x}$ $[N/m]$	f_N $[Hz]$	$M_{r,x}$ $[kg]$
500	1.2	8.8
2500	3.0	7.0
5000	4.3	6.8

General Notation

B. ADAPTIVE INTERACTION CONTROL DESIGN

- $\mathbf{f}$: vector of measured robot forces
- $\mathbf{f}^d$: vector of reference robot forces
- $\mathbf{f}^f$: vector of reference filtered robot forces
- LPF: low pass filter with user-defined bandwidth ω_f
- $\mathbf{e}_f$: force error vector, $\mathbf{e}_f = \mathbf{f}^f - \mathbf{f}$
- $\mathbf{G}_{pf}$: diagonal adaptive gain matrix for force-tracking purposes
- $\mathbf{G}_h$: diagonal adaptive gain matrix for additional damping ratio calculation

The control law here presented (Figure 3) aims at on-line adapt the impedance control set-point in order to track a reference force during the execution of an interaction task (*e.g.*, assembly task), while avoiding force-overshoots (that may compromise the task execution) and compensating the compliant robot base dynamics (that affects the interaction at the robot end-effector). On the basis of the reference force $\mathbf{f}^d$, its filtered value $\mathbf{f}^f$ (obtained by processing the reference force $\mathbf{f}^d$ with a low pass filter LPF) and the measured force $\mathbf{f}$, an adaptive proportional control gain matrix $\mathbf{G}_{pf}$ is, therefore, defined in order to achieve the target force-tracking capabilities (*i.e.*, track the reference force $\mathbf{f}^d$ while avoiding force overshoots and compensating the compliant robot dynamics):

$$\mathbf{G}_{pf}(i,i) = \alpha \int (1 - \mid \mathbf{f}(i) \mid / \mid \mathbf{f}^d(i) \mid) \mid \mathbf{f}^f(i) \mid \delta t \tag{4}$$

where i identifies the update of a the i^{th} diagonal element and α is a deformation gain for the calculus of $\mathbf{G}_{pf}$.

On the basis of the reference force $\mathbf{f}^d$ and the measured force $\mathbf{f}$, an adaptive derivative control gain matrix $\mathbf{G}_h$ is defined in order to adapt the damping of the closed-loop. The main idea is to have an increasing damping contribution while the reference force is reached. Therefore, the adaptive derivative control gain matrix $\mathbf{G}_h$ can be defined as follows:

$$\mathbf{G}_h(i,i) = h_0(\mathbf{f}(i)/\mathbf{f}^d(i)); \tag{5}$$

where h_0 is the target additional damping to be implemented when the reference force $\mathbf{f}^d$ is tracked.

The impedance control set-point is then defined as follows:

$$\mathbf{x}^0_r = \mathbf{x}_r + \mathbf{G}_{pf}\mathbf{e}_f - \mathbf{K}_r^{-1}\mathbf{G}_D\dot{\mathbf{x}}_r + \mathbf{K}_r^{-1}\mathbf{f}^f \tag{6}$$

where $\mathbf{G}_D = 2\sqrt{\mathbf{K}_r\mathbf{M}_r}\mathbf{G}_h$ is the adaptive damping on-line calculated and $\mathbf{K}_r^{-1}\mathbf{f}^f$ is a feedforward term.

The developed control schema does not need to identify the dynamic model of the interacting environment, neither the model of the compliant robot base. In fact, based on the definition of $\mathbf{G}_{pf}$ in (4) and $\mathbf{G}_h$ in (5), the impedance control set-point $\mathbf{x}^0_r$ is adapted on-line to obtain the target performance.

The proposed control schema is applied to the traslational DoFs, while rotational DoFs set-point is kept constant as in many industrial tasks (*e.g.*, assembly tasks, polishing tasks).

III. CONTROLLER STABILITY ANALYSIS

A. INTERACTION DYNAMICS MODELING

To prove the stability of the proposed controller, the linear interaction dynamics shown in Figure 4 has been taken into account in the following. The proposed controller has also been experimentally validated in Section IV taking into account non-linear compliant robot bases and interacting environment.

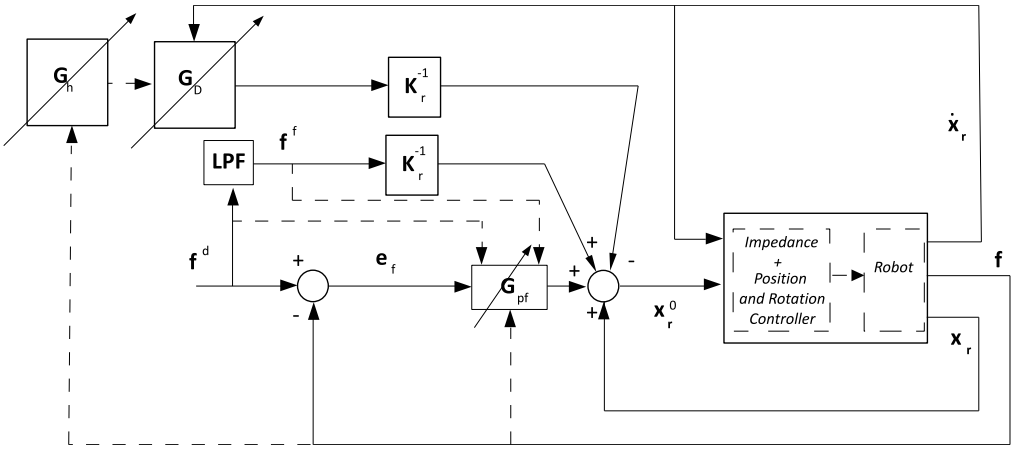

FIGURE 3. Adaptive control schema showing the control parameters calculation and the impedance control set-point updating law.

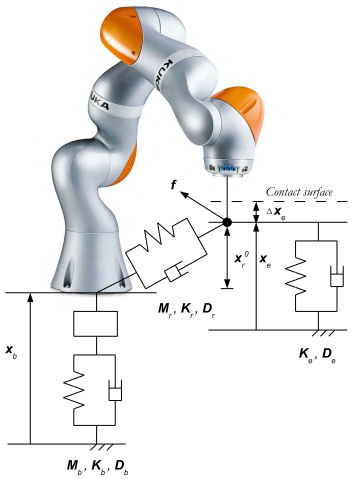

FIGURE 4. Linear interaction dynamics model, highlighting the robot impedance control model, the environment model and the compliant robot base model.

1) COMPLIANT ENVIRONMENT DYNAMICS

Denoting $\mathbf{x}_e$, $\mathbf{D}_e$ and $\mathbf{K}_e$ as the environment position, damping and stiffness, a simplified environment dynamics can be modeled as [31]:

$$\mathbf{D}_e\dot{\mathbf{x}}_e + \mathbf{K}_e\,\Delta\mathbf{x}_e = \mathbf{f}_e \tag{7}$$

where $\mathbf{x}_e^0 = \mathbf{x}_e - \mathbf{x}_e^0$ the equilibrium position for the environment, and $\mathbf{f}_e$ is the force exerted on the environment. Without loss of generality, the equilibrium position of the environment can be imposed equal to zero, *i.e.*, $\mathbf{x}_e^0 = 0$.

Such model considers local small deformations of the interacting environment and small/limited accelerations (*i.e.*, $\ddot{\mathbf{x}}_e \longrightarrow 0$, negligible inertia term). The acceleration $\ddot{\mathbf{x}}_e$ (and the inertia term related to $\mathbf{M}_e$) can be taken into account in the environment model if needed.

2) COMPLIANT ROBOT BASE DYNAMICS

Considering that light-weight manipulators can apply limited forces to a target environment (30 - 150 N, *i.e.*, introducing small deformations on the compliant structure), the robot base dynamics can be always linearized in the task operating condition. Therefore, a compliant platform can be modeled considering its relevant N eigenmodes. Moreover, considering the limited bandwidth achievable by the controller to ensure safety while executing the target task, only the dominant eigenmode (at low-frequency) is considered to model the robot base dynamics (*i.e.*, higher-frequency eigenmodes are negligible). Thus, a simple mass $\mathbf{M}_b$ - spring $\mathbf{K}_b$ - damper $\mathbf{D}_b$ model describes properly the robot base dynamics [32]:

$$\mathbf{M}_b\ddot{\mathbf{x}}_b + \mathbf{D}_b\dot{\mathbf{x}}_b + \mathbf{K}_b\Delta\mathbf{x}_b = \mathbf{f}_b \tag{8}$$

where $\mathbf{x}_b^0 = \mathbf{x}_b - \mathbf{x}_b^0$ is the equilibrium position for the robot base, and $\mathbf{f}_b$ is the interaction force between the compliant robot base and the robot. Without loss of generality, the equilibrium position of the robot base can be imposed equal to zero, *i.e.*, $\mathbf{x}_b^0 = 0$.

Such model can be extended also to mobile platforms. In fact, interaction tasks (such as assembly, disassembly, sampling, polishing, drilling tasks) are commonly operated by stopping the mobile platform (*i.e.*, by braking the wheels). In such configuration, the elasticity introduced by the mobile platform (the series of the main body, wheel structure, tyre) can be modeled as an equivalent mass - spring - damper system to the purpose of the interaction control according to the above assumption. An approach considering a mass - spring - damper modeling of the tyre - soil system can be found in [33].

3) COUPLED DYNAMICS

The following assumptions are considered:

Assumption 1: Small rotations are considered such that the environment pose results in $\mathbf{x}_e = \mathbf{x}_b + \mathbf{x}_r$. This assumption is valid in many interaction tasks, such as assembly, disassembly, sampling, polishing, drilling tasks, where the task is mainly defined in a target direction.

Assumption 2: The energy dissipation at the contact is neglectable such that the exchanged forces at interaction

points remain unaltered (*i.e.*, $\mathbf{f}_r = -\mathbf{f}_e = -\mathbf{f}$), and the accelerations of the robot mass are neglectable.

Assumption 3: The dynamic parameters ($\mathbf{M}_b$, $\mathbf{K}_b$, $\mathbf{D}_b$, $\mathbf{K}_e$, $\mathbf{D}_e$) are either constant or varying at low rate (at least one decade lower than the response of the controlled system).

Assumption 4: Based on Section II-A, the Cartesian impedance controller can be modeled as a 6 DoFs decoupled mass - spring - damper system. Therefore, even considering a compliant robot mounting, the controlled manipulator parameters $\mathbf{M}_r$, $\mathbf{D}_r$ and $\mathbf{K}_r$ are superimposed to the classical robot dynamics by the Cartesian impedance control. In such a way, the floating robot mass is equal to $\mathbf{M}_r$ and can be concentrated at the robot end-effector. The same is applied to the controlled robot stiffness.

Assumption 5: The robot base mass $\mathbf{M}_b$ is defined only by the moving parts composing to the compliant robot mounting.

The coupled system dynamics takes into account the absolute position $\mathbf{x}_b$ of the compliant robot base and the relative position of the robot $\mathbf{x}_r$ with respect to $\mathbf{x}_b$ as DoFs. The potential energy V, the kinetic energy T and the dissipation D (quantities are referred to scalar notation; the extension to matrix notation is straightforward having a decoupled system) can then be derived:

$$\begin{aligned} V &= \frac{1}{2}K_e\left(x_b + x_r - x_e^0\right)^2 + \frac{1}{2}K_b\left(x_b - x_b^0\right)^2 \\ &\quad + \frac{1}{2}K_r\left(x_r - x_r^0(x_r, x_b)\right)^2 \\ T &= \frac{1}{2}M_r\left(\dot{x}_b + \dot{x}_r\right)^2 + \frac{1}{2}M_b\left(\dot{x}_b\right)^2 \\ D &= \frac{1}{2}D_e\left(\dot{x}_b + \dot{x}_r\right)^2 + \frac{1}{2}D_r\left(\dot{x}_r\right)^2 + \frac{1}{2}D_b\left(\dot{x}_b\right)^2 \end{aligned} \tag{9}$$

Thus, under the defined assumptions, applying the Lagrangian approach [34], the coupled dynamics of Figure 4 results in (considering the matrix expression):

$$\begin{cases} 0 = \mathbf{M}_r(\ddot{\mathbf{x}}_r + \ddot{\mathbf{x}}_b) + \mathbf{M}_b\ddot{\mathbf{x}}_b + \mathbf{D}_b\dot{\mathbf{x}}_b \\ \quad + \mathbf{D}_e\left(\dot{\mathbf{x}}_b + \dot{\mathbf{x}}_r\right) - \mathbf{K}_r(\mathbf{x}_r - \mathbf{x}_r^0)\dfrac{\partial \mathbf{x}_r^0}{\partial \mathbf{x}_b} \\ \quad + \mathbf{K}_b(\mathbf{x}_b - \mathbf{x}_b^0) + \mathbf{K}_e\left(\mathbf{x}_b + \mathbf{x}_r - \mathbf{x}_e^0\right) \\ 0 = \mathbf{M}_r(\ddot{\mathbf{x}}_r + \ddot{\mathbf{x}}_b) + \mathbf{D}_r\dot{\mathbf{x}}_r \\ \quad + \mathbf{D}_e\left(\dot{\mathbf{x}}_b + \dot{\mathbf{x}}_r\right) + \mathbf{K}_e\left(\mathbf{x}_b + \mathbf{x}_r - \mathbf{x}_e^0\right) \\ \quad + \mathbf{K}_r(\mathbf{x}_r - \mathbf{x}_r^0)(1 - \dfrac{\partial \mathbf{x}_r^0}{\partial \mathbf{x}_r}) \end{cases} \tag{10}$$

B. LIAPUNOV STABILITY

Considering a single Cartesian DoF (*i.e.*, scalar quantities since the Cartesian impedance control allows to decouple the Cartesian DoFs), the Lyapunov stabilities conditions have to be satisfy in order to prove the closed-loop system stability. On the basis of (9), the positive scalar Lyapunov function candidate is defined as:

$$V_{Ly} = T + V \tag{11}$$

The Lyapunov function candidate is therefore defined as:

$$\begin{aligned} V_{Ly} &= \frac{1}{2}M_r\left(\dot{x}_b + \dot{x}_r\right)^2 + \frac{1}{2}M_b\left(\dot{x}_b\right)^2 \\ &\quad + \frac{1}{2}K_e\left(x_b + x_r - x_e^0\right)^2 + \frac{1}{2}K_b\left(x_b - x_b^0\right)^2 \\ &\quad + \frac{1}{2}K_r\left(x_r - x_r^0(x_r, x_b)\right)^2 \end{aligned} \tag{12}$$

V_{Ly} has to satisfy the first Lyapunov stability condition:

$$V_{Ly} \geq 0 \tag{13}$$

Since all the quantities in (12) are in a quadratic form and stiffness/mass matrices are positive definite, (13) is satisfied.

The derivative $\dot{V}_{Ly}$:

$$\dot{V}_{Ly} = -\left[D_e\left(\dot{x}_r + \dot{x}_b\right) + D_b\dot{x}_b\right]\dot{x}_b - \left[D_e\left(\dot{x}_r + \dot{x}_b\right) + D_r\dot{x}_r\right]\dot{x}_r \tag{14}$$

has to satisfy the second Lyapunov stability condition:

$$\dot{V}_{Ly} < 0 \tag{15}$$

(14) can be write as follows:

$$\dot{V}_{Ly} = -(D_e + D_b)\dot{x}_b^2 - (D_e + D_r)\dot{x}_r^2 - 2D_e\dot{x}_r\dot{x}_b < 0 \tag{16}$$

Considering the linearization of the first equation in (10) (that can be computed at each time step taking into account the current state of the manipulator), we can define the transfer function $G(s)$ between x_b and x_r and its inverse Laplace transform $H(t)$:

$$\frac{X_b(s)}{X_r(s)} = G(s), \quad H(t) = \mathcal{L}^{-1}\{G(s)\} \tag{17}$$

The inverse transform of $X_b(s)$ is therefore:

$$x_b(t) = (H * x_r)(t) = \int_{-\infty}^{+\infty} H(\tau)x_r(t - \tau)\delta\tau \tag{18}$$

Using Tonelli's theorem it is possible to write:

$$\| H * x_r \|_p \leq \| H \|_1 \| x_r \|_p, \quad \forall 1 \leq p \leq \infty \tag{19}$$

The norm $\| H \|_1$ corresponds to the maximum value $\overline{M}$ of the inverse transform of (17), that we can evaluate based on the parameters of the global system we are working with. Moreover, having a limitation $\overline{x}_r$ on x_r (imposed by limiting the control action of the impedance control) we obtain:

$$\| H \|_1 \| x_r \|_p = \overline{M}\overline{x}_r \tag{20}$$

Defining $Z = \dfrac{\dot{x}_r}{\| \dot{x}_r \|_p}$ and the definition in (20), the second Lyapunov condition has to be satisfied referring to the new Z variable:

$$(D_e + D_r)Z^2 + 2D_e\overline{M}Z + (D_e + D_b)\overline{M}^2 > 0 \tag{21}$$

Such condition can be easily satisfy by imposing the impedance control damping D_r in order to have a critical damped impedance control behavior. A procedure to automatize the updating of the impedance control damping D_r in case of instabilities generation can also be designed.

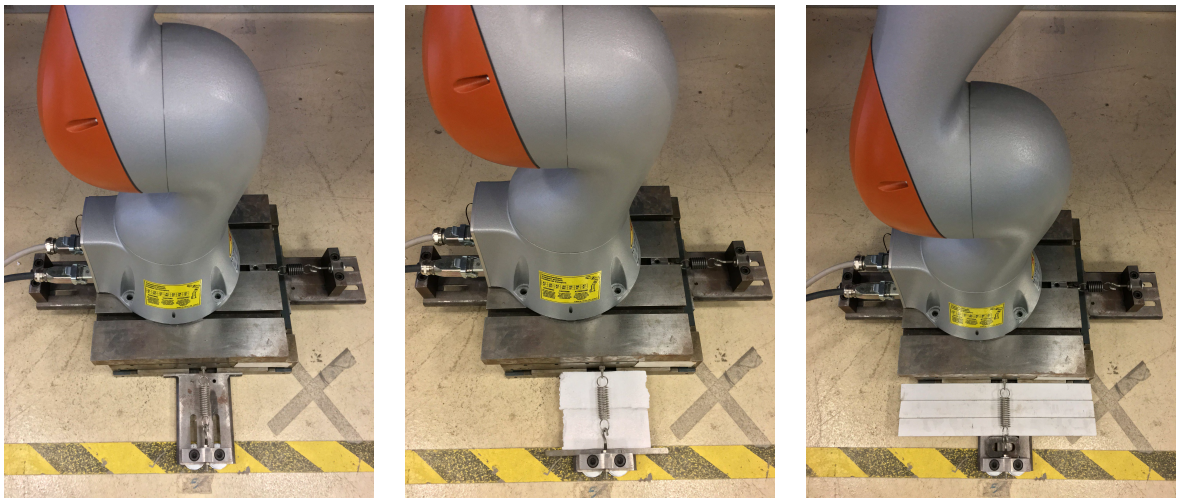

FIGURE 5. The three experimental setup are shown in the Figure: (a) linear robot base dynamics, (b) continuous non-linear robot base dynamics, (c) discontinuous non-linear robot base dynamics (in such set-up, an air gap is left between the rest position of the robot base and the steel element to implement an impulsive change in the robot base dynamics).

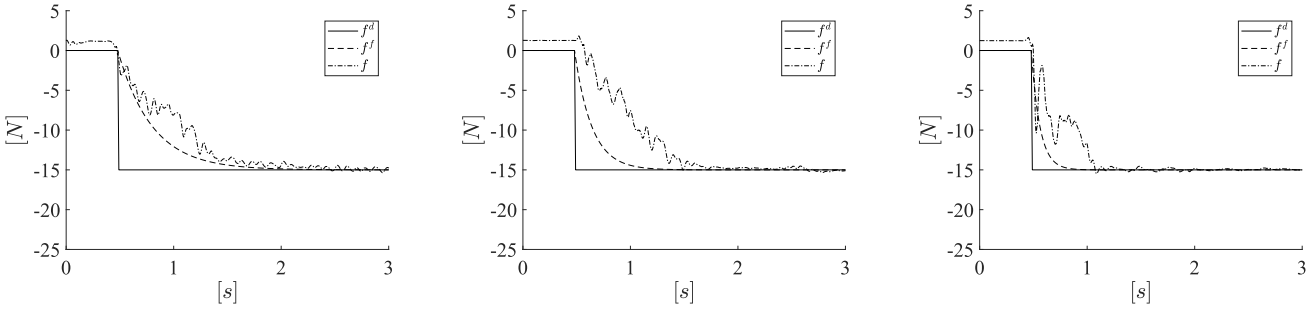

FIGURE 6. Reference force f^d, filtered reference force f^f and measured force f are shown taking into account the compliant robot base configuration shown in figure 5 (a). (a) $\omega_f = 3.14[rad/s]$ (*i.e.*, frequency of 0.5[*Hz*]), (b) $\omega_f = 6.28[rad/s]$ (*i.e.*, frequency of 1[*Hz*]), (c) $\omega_f = 12.56[rad/s]$ (*i.e.*, frequency of 2[*Hz*]).

IV. EXPERIMENTAL VALIDATION

A. SETUP DESCRIPTION

An assembly task (Figure 1) has been considered for the control validation. The assembly application has a main task direction (X direction), common situation in many industrial tasks. A KUKA iiwa 14 R820 manipulator equipped with a Robotiq gripper as been used as a test-platform. The KUKA iiwa 14 R820 has been mounted on a compliant base, implementing three different behaviors (Figure 5): (a) linear dynamics (obtained using a linear spring with $K_{b,x} = 4000[N/m]$), (b) continuous non-linear dynamics (obtained using a parallel system composed by a linear spring and by a styrofoam element), (c) discontinuous non-linear dynamics (obtained by a linear spring and by a steel element to implement an impulsive change in the robot base dynamics).

The following control parameters has been used: $\alpha = 0.1$, $h_0 = 0.25, f^d = -15[N]$. Three different values for the force filter bandwidth ω_f has been imposed in order to evaluate the proposed controller: $\omega_f = [3.14, 6.28, 12.56][rad/s]$.

Experimental results are described in the following Section.

B. RESULTS

Figure 6 shows the interaction forces with respect to the experimental set-up shown in Figure 5 (a). The plots show the tracking performance of the proposed controller, capable to avoid any overshoot while achieving the target bandwidth specified by ω_f.

Figure 7 shows the interaction forces with respect to the experimental set-up shown in Figure 5 (b). The plots show the tracking performance of the proposed controller. Only the plot related to $\omega_f = 12.56[rad/s]$ shows a limited force overshoot.

Figure 8 shows the interaction forces with respect to the experimental set-up shown in Figure 5 (c). The plots

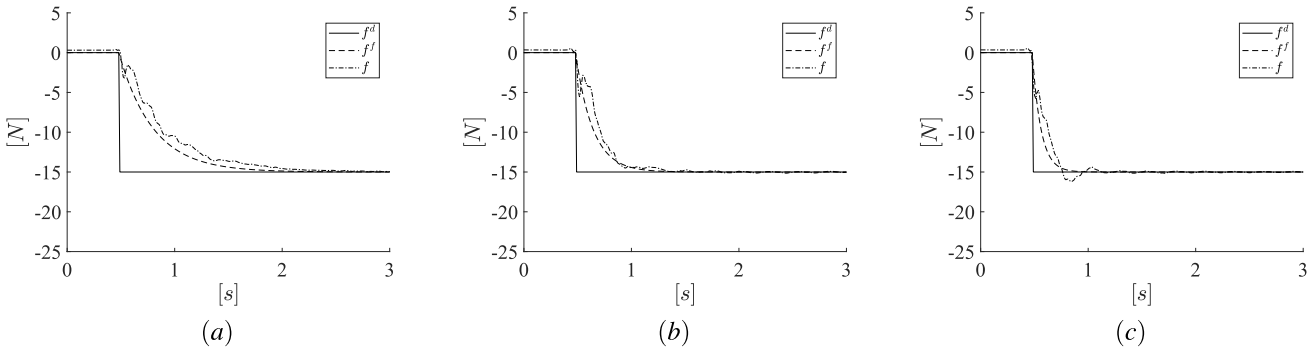

FIGURE 7. Reference force f^d, filtered reference force f^f and measured force f are shown taking into account the compliant robot base configuration shown in figure 5 (b). (a) $\omega_f = 3.14[rad/s]$ (*i.e.*, frequency of 0.5[*Hz*]), (b) $\omega_f = 6.28[rad/s]$ (*i.e.*, frequency of 1[*Hz*]), (c) $\omega_f = 12.56[rad/s]$ (*i.e.*, frequency of 2[*Hz*]).

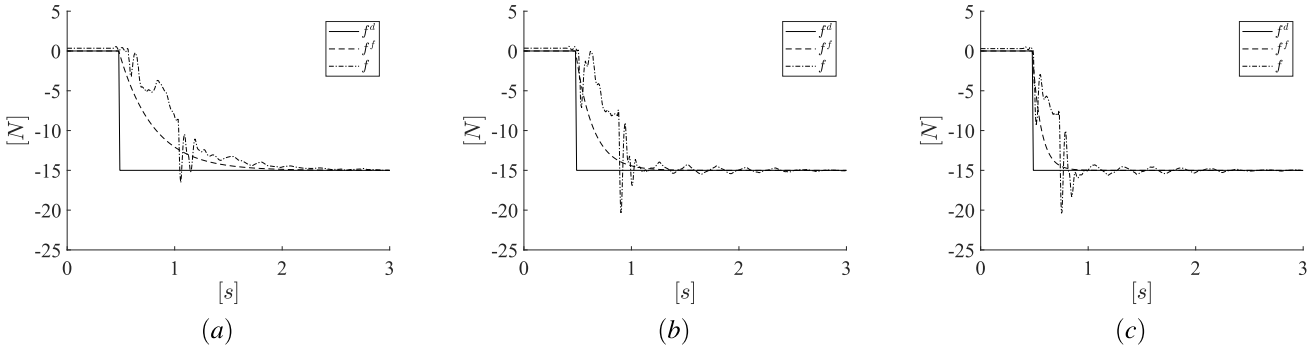

FIGURE 8. Reference force f^d, filtered reference force f^f and measured force f are shown taking into account the compliant robot base configuration shown in figure 5 (c). (a) $\omega_f = 3.14[rad/s]$ (*i.e.*, frequency of 0.5[*Hz*]), (b) $\omega_f = 6.28[rad/s]$ (*i.e.*, frequency of 1[*Hz*]), (c) $\omega_f = 12.56[rad/s]$ (*i.e.*, frequency of 2[*Hz*]).

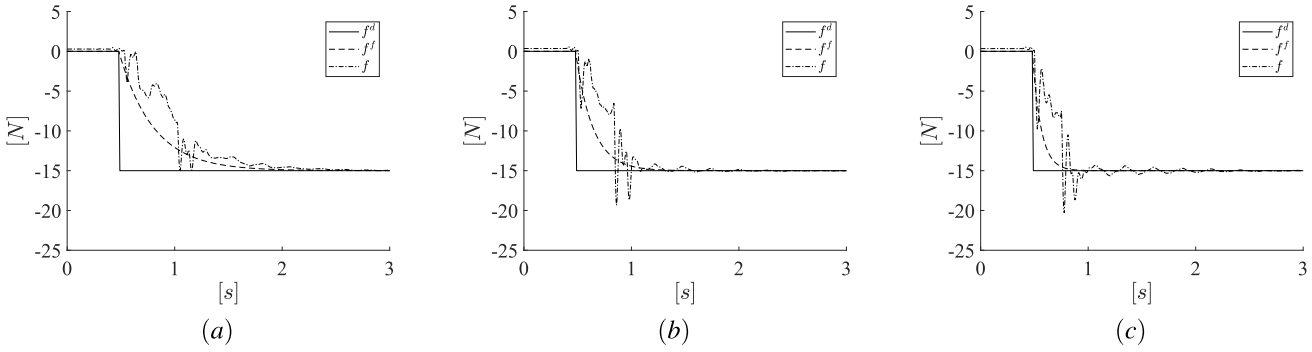

FIGURE 9. Reference force f^d, filtered reference force f^f and measured force f are shown taking into account the compliant robot base configuration shown in figure 5 (c) and imposing a reduced value for the control gain $\alpha = 0.01$. (a) $\omega_f = 3.14[rad/s]$ (*i.e.*, frequency of 0.5[*Hz*]), (b) $\omega_f = 6.28[rad/s]$ (*i.e.*, frequency of 1[*Hz*]), (c) $\omega_f = 12.56[rad/s]$ (*i.e.*, frequency of 2[*Hz*]).

show the tracking performance of the proposed controller. Force overshoots are displayed, while stability is achieved. In order to reduce/avoid force overshoots, the control parameter $\alpha = 0.01$ has been used in the same experiment and the related experimental results are shown in Figure 9. Plot (a) shows the force overshoots avoidance, while plots (b) and (c) show a reduction of the force overshoots.

C. RESULTS COMPARISON WITH PREVIOUS DESIGNED METHODS

In this Sections, obtained control performance are compared with previous developed controllers.

In [25] the force overshoots issue has not been taken into account in the developed controller. Although the proposed control method is capable to track a target force reference while compensating for the compliant robot

base dynamics, force overshoots are shown in the experimental results.

In [14] and [26] the force overshoot issue has been taken into account only considering a linear dynamics modeling the interacting environment and the compliant robot base. Moreover, both the control methods require the estimation of the interaction dynamics parameters, increasing the complexity of the proposed methodology and requiring external sensors to perform the identification procedure (*e.g.*, accelerometers). In addition, the control performance are, therefore, affected by such parameters estimation.

Comparing the performance of the here proposed controller with the controller in [14], it can be highlighted that the achievable closed-loop bandwidth has been improved. In fact, experimental results in [14] show a maximum closed-loop bandwidth of 0.66 *Hz*. The here proposed method allows to achieved a closed-loop bandwidth of 2 *Hz* with the same experimental setup.

Therefore, the here proposed control allows to improve the control performance while avoiding any estimation of the interaction dynamics parameters and any use of external additional sensor. In such a way, the control performance are not affected by external observers or models. Moreover, the proposed method allows to adapt the control gains during the task execution, achieving the target control performance even considering an evolving interaction dynamics.

V. CONCLUSIONS

In this paper, an adaptive interaction controller has been proposed in order to deal with a compliant base unknown dynamics. Avoiding any estimation of the environment dynamics, neither of the compliant robot base dynamics, the proposed controller is capable to on-line adapt its behavior, achieving the tracking of a force reference. The impedance control setpoint is on-line calculated, adapting the control parameters on the basis of the measured interaction. The stability of the proposed controller has been theoretically proven and experimental results show the controller performance (considering linear and non-linear robot base dynamics). Results have also been compared with previous developed control strategies, highlighting the improved control performance.

Future work will consider visual servoing to improve the autonomy of the manipulator. In such a way, a position feedback can also be included in the control law in order to correct the robot positioning during the assembly execution. Moreover, mobile platforms will be taken into account and the control algorithm will be extended to a human-robot co-operative application (*e.g.*, a co-manipulation task).

ACKNOWLEDGMENT

The authors would like to thank T. Dinon (CNR-STIIMA) for expertise and support.

REFERENCES

[1] L. Roveda, N. Iannacci, F. Vicentini, N. Pedrocchi, F. Braghin, and L. M. Tosatti, "Optimal impedance force-tracking control design with impact formulation for interaction tasks," *IEEE Robot. Autom. Lett.*, vol. 1, no. 1, pp. 130–136, Jan. 2016.

[2] P. J. From, J. T. Gravdahl, and K. Y. Pettersen, *Vehicle-Manipulator Systems*. London, U.K.: Springer, 2014.

[3] E. Colgate and N. Hogan, "The interaction of robots with passive environments: Application to force feedback control," in *Advanced Robotics*. Berlin, Germany: Springer, 1989, pp. 465–474.

[4] N. Hogan, "Impedance control: An approach to manipulation," in *Proc. Amer. Control Conf.*, Jun. 1984, pp. 304–313.

[5] C. Ott, R. Mukherjee, and Y. Nakamura, "Unified impedance and admittance control," in *Proc. IEEE Int. Conf. Robot. Automat. (ICRA)*, May 2010, pp. 554–561.

[6] H. Seraji and R. Colbaugh, "Force tracking in impedance control," *Int. J. Robot. Res.*, vol. 16, no. 1, pp. 97–117, Feb. 1997.

[7] S. Jung, T. C. Hsia, and R. G. Bonitz, "Force tracking impedance control of robot manipulators under unknown environment," *IEEE Trans. Control Syst. Technol.*, vol. 12, no. 3, pp. 474–483, May 2004.

[8] L. Roveda, N. Pedrocchi, and L. M. Tosatti, "Exploiting impedance shaping approaches to overcome force overshoots in delicate interaction tasks," *Int. J. Adv. Robotic Syst.*, vol. 13, no. 5, p. 1729881416662771, 2016.

[9] R. Ikeura and H. Inooka, "Variable impedance control of a robot for cooperation with a human," in *Proc. IEEE Intl. Conf. Robot. Autom. (ICRA)*, vol. 3, May 1995, pp. 3097–3102.

[10] F. Ficuciello, L. Villani, and B. Siciliano, "Variable impedance control of redundant manipulators for intuitive human–robot physical interaction," *IEEE Trans. Robot.*, vol. 31, no. 4, pp. 850–863, Aug. 2015.

[11] G. Dudek and M. Jenkin, *Computational Principles of Mobile Robotics*. Cambridge, U.K.: Cambridge Univ. Press, 2010.

[12] P. J. From, I. Schjølberg, J. T. Gravdahl, K. Y. Pettersen, and T. I. Fossen, "On the boundedness property of the inertia matrix and skew-symmetric property of the coriolis matrix for vehicle-manipulator systems," *J. Dyn. Syst., Meas., Control*, vol. 134, no. 4, p. 044501, 2012.

[13] S. Erhart, D. Sieber, and S. Hirche, "An impedance-based control architecture for multi-robot cooperative dual-arm mobile manipulation," in *Proc. IEEE/RSJ Int. Conf. Intell. Robots Syst. (IROS)*, Nov. 2013, pp. 315–322.

[14] L. Roveda, N. Pedrocchi, F. Vicentini, and L. M. Tosatti, "An interaction controller formulation to systematically avoid force overshoots through impedance shaping method with compliant robot base," *Mechatronics*, vol. 39, pp. 42–53, Nov. 2016.

[15] L. T. Le, "Passivity based on energy tank for Cartesian impedance control of DLR space robots with floating base and elastic joints," *J. Comput. Sci. Cybern.*, vol. 34, no. 1, pp. 49–62, 2018.

[16] K. Yoshida, D. N. Nenchev, and M. Uchiyama, "Moving base robotics and reaction management control," in *Robotics Research*, G. Giralt and G. Hirzinger, Eds. London, U.K.: Springer, 2000, pp. 100–109.

[17] J. Y. Lew and S. M. Moon, "A simple active damping control for compliant base manipulators," *IEEE/ASME Trans. Mechatronics*, vol. 6, no. 3, pp. 305–310, Sep. 2001.

[18] M. Reyhanoglu and D. Hoffman, "Finite-time control of a compliant base robot manipulator," in *Proc. 11th Asian Control Conf. (ASCC)*, Dec. 2017, pp. 1335–1340.

[19] J. Y. Lew, "Contact control of flexible micro/macro-manipulators," in *Proc. IEEE Int. Conf. Robot. Automat.*, vol. 4, Apr. 1997, pp. 2850–2855.

[20] C. Ott, A. Albu-Schaffer, and G. Hirzinger, "A Cartesian compliance controller for a manipulator mounted on a flexible structure," in *Proc. IEEE/RSJ Int. Conf. Intell. Robots Syst.*, Oct. 2006, pp. 4502–4508.

[21] T. Wongratanaphisan and M. O. T. Cole, "Robust impedance control of a flexible structure mounted manipulator performing contact tasks," *IEEE Trans. Robot.*, vol. 25, no. 2, pp. 445–451, Apr. 2009.

[22] L. Roveda, F. Vicentini, and L. M. Tosatti, "Deformation-tracking impedance control in interaction with uncertain environments," in *Proc. IEEE/RSJ Int. Conf. Intell. Robots Syst. (IROS)*, Nov. 2013, pp. 1992–1997.

[23] L. Roveda, F. Vicentini, N. Pedrocchi, F. Braghin, and L. Molinari Tosatti, "Impedance shaping controller for robotic applications in interaction with compliant environments," in *Proc. 11th Int. Conf. Inform. Control, Automat. Robot. (ICINCO)*, vol. 2, Sep. 2014, pp. 444–450.

[24] L. Roveda, F. Vicentini, N. Pedrocchi, and L. M. Tosatti, "Impedance control based force-tracking algorithm for interaction robotics tasks: An analytically force overshoots-free approach," in *Proc. 12th Int. Conf. Inform. Control, Automat. Robot. (ICINCO)*, Jul. 2015, pp. 386–391.

[25] L. Roveda, F. Vicentini, N. Pedrocchi, and L. M. Tosatti, "Force-tracking impedance control for manipulators mounted on compliant bases," in *Proc. IEEE Int. Conf. Robot. Automat. (ICRA)*, May/Jun. 2014, pp. 760–765.

[26] L. Roveda, F. Vicentini, N. Pedrocchi, F. Braghin, and L. M. Tosatti, "Impedance shaping controller for robotic applications involving interacting compliant environments and compliant robot bases," in *Proc. IEEE Int. Conf. Robot. Automat. (ICRA)*, May 2015, pp. 2066–2071.
[27] L. Sciavicco and B. Siciliano, *Modelling and Control of Robot Manipulators*. New York, NY, USA: Springer, 2012.
[28] B. Siciliano and L. Villani, *Robot Force Control*, 1st ed. Norwell, MA, USA: Kluwer, 2000.
[29] A. Albu-Schäffer, C. Ott, and G. Hirzinger, "A unified passivity-based control framework for position, torque and impedance control of flexible joint robots," *Int. J. Robot. Res.*, vol. 26, no. 1, pp. 23–39, 2007.
[30] L. Roveda, "Model based compliance shaping control of light-weight manipulator in hard-contact industrial applications," Ph.D. dissertation, Mech. Eng. Dept., Politecnico di Milano, Milan, Italy, 2015.
[31] W. Flügge, *Viscoelasticity*. New York, NY, USA: Springer 1975.
[32] D. N. Nenchev, K. Yoshida, P. Vichitkulsawat, and M. Uchiyama, "Reaction null-space control of flexible structure mounted manipulator systems," *IEEE Trans. Robot. Autom.*, vol. 15, no. 6, pp. 1011–1023, Dec. 1999.
[33] S. Taheri, C. Sandu, S. Taheri, E. Pinto, and D. Gorsich, "A technical survey on Terramechanics models for tire–terrain interaction used in modeling and simulation of wheeled vehicles," *J. Terramech.*, vol. 57, pp. 1–22, Feb. 2015.
[34] L. Sciavicco and B. Siciliano, *Modelling and Control of Robot Manipulators*. London, U.K: Springer, 2000.

LORIS ROVEDA received the B.S., M.S., and Ph.D. degrees in mechanical engineering from the Politecnico di Milano, Milan, Italy, in 2009, 2011, and 2015, respectively.

Since 2015, he has been a Research with the Institute of Intelligent Industrial Technologies and Systems for Advanced Manufacturing, Italian National Research Council. He is the author of international publications. He is involved in many European projects, including H2020 CS2 EURECA. His research interests include human–robot cooperation, interaction control for autonomous industrial tasks, design and control of robots, and wearable robotics.